Laser Propulsion Research Facilities at DLR Stuttgart

Stephanie Karg, Vitalij Fedotov, Torben Sehnert and Hans-Albert Eckel

Institute of Technical Physics, German Aerospace Center (DLR), D-70569 Stuttgart, Pfaffenwaldring 38 - 40, Germany

Abstract. Irradiation of materials with sufficiently high laser fluence induces an ablation process at the surface yielding a plasma jet of ablated material and laser-induced force acting on the material due to the recoil of the jet. The paper gives an overview of DLR's experimental facilities for investigation of the potential of laser ablation induced thrust for future microthrusters and space debris removal. A thrust balance based on a modular torsional pendulum concept and suitable calibration facilities have been constructed for μN to mN measurements in vacuum. In addition, modification of the sample surface after ablation is determined by using a white light interferometry profiler. Moreover, divergence and velocity distribution of ions in the ablation plume are investigated by angularly resolved Faraday cup measurements.

Keywords: Laser ablation of solids, Laser ablation microthruster, Plasma diagnostic techniques
PACS: 52.70.-m, 79.20.Eb

1 INTRODUCTION

Impulse imparted by pulsed laser ablation of a thin layer of material creating a plasma or vapor is an interesting concept that allows for scaling of the induced thrust over a large range by selecting an ablation laser of appropriate pulse energy and repetition rate. Its potential for the removal of space debris using a high energy laser [1, 2] and for laser ablative microthrusters which produce highly precise thrust in the μN range at μJ to mJ pulse energies [3, 4] has been investigated. This paper provides an overview of the research facilities, which have been set up at DLR Stuttgart to further investigate the potential of both of these applications of laser ablative propulsion.

It has been demonstrated that laser ablative thrusters can produce μN thrust levels at high specific impulse and have the capability of producing very low minimum impulse bits down to nNs range in single shot operation [3, 4]. So far these concepts have been based on providing unablated material at each laser pulse by implementing a propellant feed mechanism [3, 5] or using a liquid propellant [6]. An additional feature that we aim to introduce in our thruster concept is to avoid moving parts by using electro-optical beam steering and layer-by-layer ablation of a solid target material (for more details see [7]). Important research and development issues are: ensuring a precisely controllable thrust level, sufficient thruster lifetime and optimization of layer-by-layer ablation that could affect satellite operation e.g. contamination issues.

Laser based systems for detection and removal of small space debris objects are being

developed in cooperation with international partners [1, 8]. The goal is to reduce a debris object's desorbitation time by lowering its perigee by means of impulse imparted by laser ablation with a high energy laser. As part of these research activities the magnitude and direction of the impulse that is imparted by illuminating a large area or even the whole debris object is being investigated. Additionally to studies of the impulse coupling coefficient for different types of debris relevant materials, the effect of debris geometry and orientation when illuminating a larger debris part have to be taken into account.
The paper gives an overview of the research facilities that have been established at DLR Stuttgart. First an overview of the underlying research strategy is given, then the experimental facilities are discussed in more detail and finally an outlook on future plans is given.

2 STRATEGY OVERVIEW

According to the goals that have been discussed in the introduction, a research strategy for laser ablative propulsion has been structured according to the outline given in Fig. 1. This strategy and the laboratory facilities have originally been devised with the aim of microthruster development and this will be the main focus of the discussion. It can, however, also be applied to laser propulsion research for space debris removal.

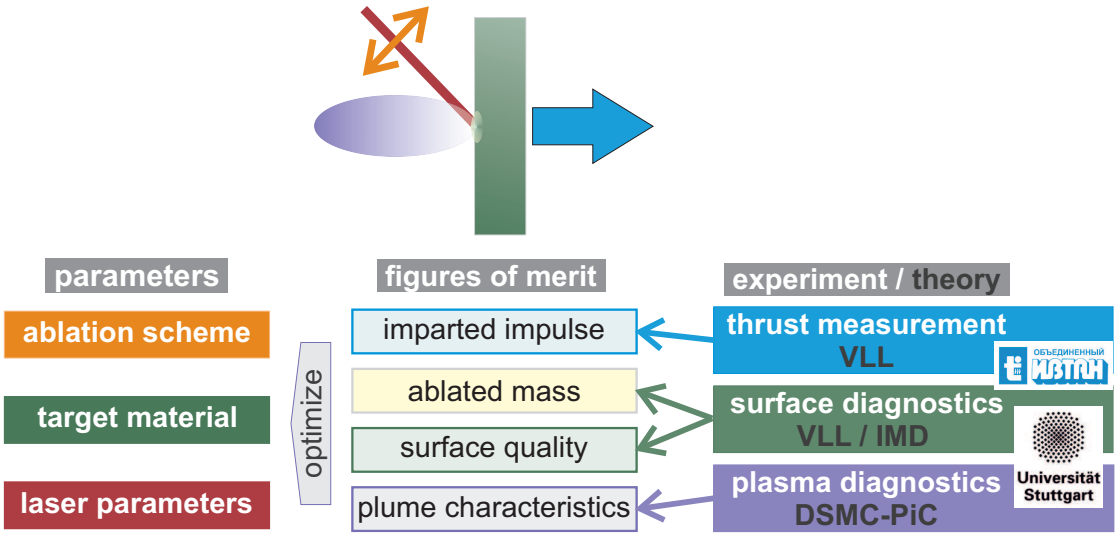

FIGURE 1. Overview of laser propulsion research strategy.

Figures of merit

The usual figures of merit given for laser ablative thrusters are the impulse coupling coefficient defined as $c_m = \frac{\Delta P}{E} = \frac{\Delta m \cdot v_{jet}}{E}$ and specific impulse $I_{sp} = \frac{v_{jet}}{g}$. Where ΔP is the imparted impulse, E the laser pulse energy, Δm the ablated mass, v_{jet} the average jet

velocity and g the gravitational acceleration. Thus specific impulse and coupling coefficient can be determined by measuring the ablated mass, imparted impulse and pulse energy. Unlike previously implemented thruster concepts, that provide a virgin spot of target material at each laser pulse by utilizing different means of target transportation [3, 4], our no-moving parts concept does rely on layer-by-layer ablation of a bulk target. As a result the changing target surface quality and its effect on thruster performance will have to be taken into account. Plasma plume characteristics have also been identified as an additional figure of merit. They can help to gain a better understanding of the ablation process, be used to verify simulation results and can also provide information on contamination issues and influence of target surface geometry and quality. The experimental facilities outlined in section 3 of this papers have been devised to provide information on these figures of merit. For space debris removal the coupling coefficient and the influence of overall target composition and geometry are of major importance.

Parameters

Parameters that can be varied in the current experimental setup are:

ablation pattern: While the ablation pattern is of minor importance for space debris related research, it is a key issue for layer-by-layer ablation in the microthruster related research activities. Different ablation patterns can be implemented by moving the target on an x,y-stage and, alternatively, by moving the focus position of the laser beam across the target by using a mechanical galvanometer mirror beam-steering setup.

laser parameters: The influence of different laser parameters (pulse length, wavelength, polarization, fluence, angle of incidence) is of interest for both research topics. Microchip lasers are the most likely candidates for a suitable microthruster laser and are as a result the main type of laser used in the experiments. Currently three different lasers, are available: two microchip lasers with wavelength 1064 nm, Gaussian beam profile, and different pulse lengths and pulse energies: 500 ps at maximum of 80 μJ (Teem Photonics, PNP-B08010-130) and 1 ns at maximum of 1 mJ (Alphalas, pulselas-P-1064-100-HE). Additionally a stable-unstable resonator $Nd:YVO_4$ slab laser (Edgewave) that provides a broader range of pulse energies (up to 7 mJ at 5 kHz) and repetition rates (up to 40 kHz at 1.6 mJ) at 1064 nm wavelength is used for thrust measurements. Laser spot size can be varied by using different focusing lenses and the fluence is usually adjusted by using a half-wave plate and polarization cube variable attenuator. This has the additional benefit of ensuring p-polarization.

target material: To avoid out-gassing issues, that can occur with polymer propellants, metals (currently Al and Cu) are used as the target material in our laser micropropulsion research. Thrust measurements for different space relevant materials (polyimide, Si solar cell material, aluminum, multi layer material) at different fluences have been carried out as part of the European CLEANSPACE project. [1].

Facilities

As outlined in the strategy overview in Fig. 1 the experimental facilities have been designed and developed for optimization of the figures of merit that are relevant for thruster lifetime and performance. They comprise thrust measurement facilities and surface and plasma diagnostics and will be described in further detail in the next section. As indicated in the figure the research activities also include simulations and modeling that supports and supplements the experimental investigations. They are carried out in cooperation with several partners: 1D hydrodynamic simulations on laser ablation of aluminum for a range of optical parameters are carried out using the Virtual Laser Lab [9] (Russian Academy of Sciences), Molecular Dynamics (MD) simulations (IMD, University of Stuttgart) and simulations with a DSMC-PIC code (IRS, University of Stuttgart). For more details see [7].

3 EXPERIMENTAL FACILITIES

Thrust Measurement

Thrust Balance Design

Torsional pendulums are frequently used for measurement of low forces including microthruster characterization [10–14]. A thrust balance based on this type of design has been developed to fulfill the following criteria: range of measurable thrust between sub μN to approx. 1 mN, minimizing the influence of external vibrations and a flexible design that leaves room for further development and improvement of the balance. For laser ablative thrusters umbilicals (e.g. power or gas feed lines) that introduce additional noise can be avoided by installing only the target on the balance. The resulting thrust balance is depicted in Fig. 2. To allow for flexible positioning as well as easy exchange of components the balance arm has a breadboard like design. A range of flexural pivots are used as the torsional element. The pivots connect the balance arm to the balance mount. Mounts that can accept different sizes of pivots are available. Where necessary for alignment purposes a range of positioning devices has been incorporated in the design, i.e. a rotational stage on the balance mount, screws for leveling of the balance mount and the base plate and translational stages for the displacement sensor and voice coils.

To minimize the impact of external influences it is necessary to keep the center of mass as close as possible to the rotational axis of the balance. For a flexible balance design variable counterweights and a setup for adjusting the location center of mass along the balance arm are required (see Fig. 2). In z-direction this has been implemented by installing a counterweight for each component that is fixed on the balance arm. In y-direction the center of mass location can be tuned by placing the balance on a blade and adjusting counterweights that consist of two micrometer screws. For this purpose a notch has been placed on the balance arm under the center of the flexural pivot (see left inset in Fig. 2).

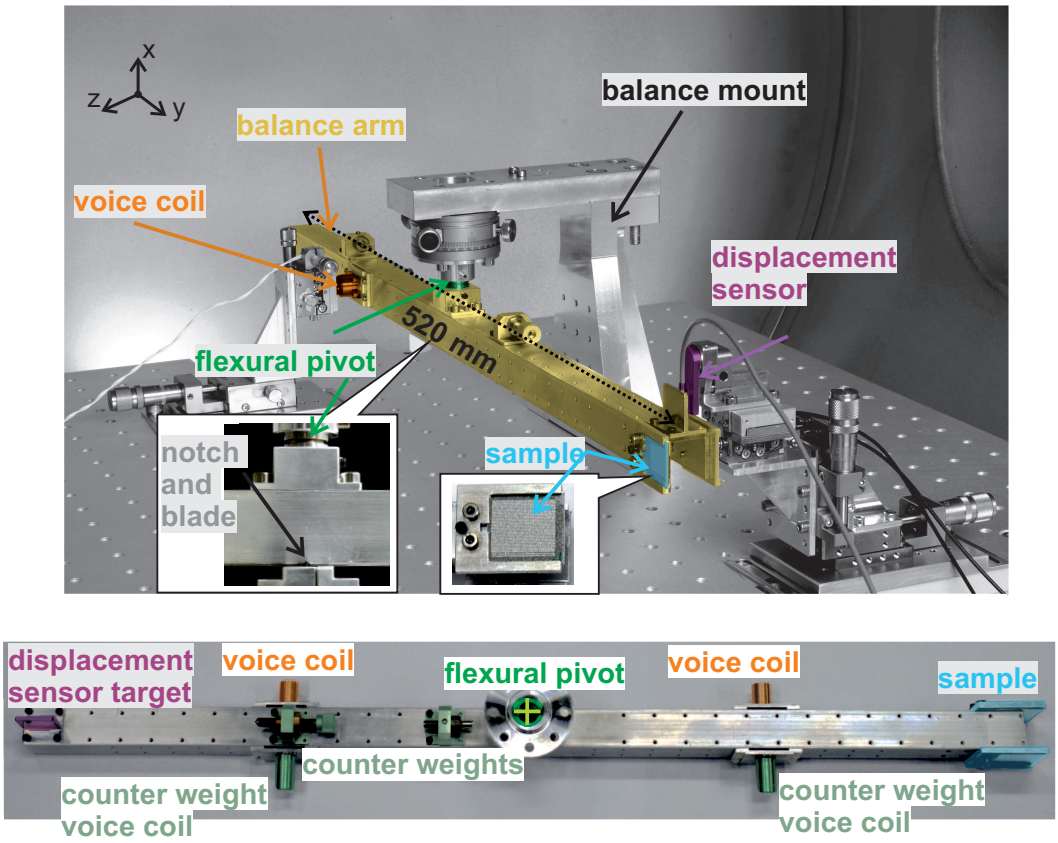

FIGURE 2. Torsional pendulum thrust balance: *top*: assembled thrust balance inside vacuum chamber, *inset (left)*: setup for CMS adjustment, *inset (right)*: sample holder; *bottom*: top view of another possible configuration of the balance arm.

The thrust balance vacuum system consists of an approx. 500 l cylindrical vacuum chamber (diameter 800 mm, length approx. 950 mm) and a pumping system consisting of a 30 m^3/h scroll pump and a 2650 l/s (N_2) magnetic bearing turbomolecular pump. To limit vibration transmission from the pumps to the chamber the backing pump line is submerged in a sandbox. The turbomolecular pump is fixed on the laboratory ceiling and attached to the chamber via a bellows connector. The vacuum chamber is installed on an optical table, which also serves as a base for the optics and beam steering setup and provides additional vibration isolation. Inside the chamber the balance assembly is installed on top of a vacuum compatible commercial vibration isolation platform (Minus K). This additional vibration isolation platform has, however, not yet been activated for actual thrust measurements.

For laser induced thrust measurements it is necessary to set up a beam-steering mechanism to provide a virgin spot of target at each shot or to implement an ablation pattern. The beam-steering setup currently used for thrust measurements is located outside

the vacuum chamber and is comprised of a galvanometer scanner and a f-theta lens (f=420 mm).

Calibration and Measurements

Voice coils are used for calibration, active damping and as a force actuator for closed-loop operation. The linear balance displacement is currently determined with a capacitive displacement measurement system that provides a linear voltage output signal. The force applied by the voice coils is controlled with a programmable DC power supply that can supply currents down to 200 μA. A multifunction data acquisition card is used to read out the capacitive sensor signal and to control the beam- steering mirrors.
The voice coils have been calibrated for a range of different coil positions using a commercial precision balance (Sartorius, CPA225D) with a repeatability of down to $\pm$0.02 mg, equivalent to 0.2 μN. The voice coils show a linear force-current characteristic for all coil positions tested in the calibration measurements and the force constant $c_{\mathrm{vc}} = 0.342\ \frac{\mu\mathrm{N}}{\mu\mathrm{A}}$ changes by less than 2% over a range of > 2 mm (see Fig. 3 a). The voice coils are positioned in the center of this range when used as a force actuator for thrust measurements.
Different measurement configurations are possible with the thrust balance: open-loop measurements with or without active damping, where thrust is measured by determining the balance displacement, and closed-loop operation, where the balance is kept in zero position by using a calibrated voice coil as a counter force actuator in a PID control loop. Here thrust is determined by measuring the current applied to the voice coil and the distance of the voice coil and thruster from the rotational axis.
Continuous thrust in open-loop configuration can be determined from a measurement of the the steady state balance displacement:

$$T = \frac{\theta_{\mathrm{final}} \cdot k}{d_{\mathrm{thr}}} \approx \frac{x_{\mathrm{final}} \cdot k}{d_{\mathrm{thr}} \cdot d_{\mathrm{capa}}} \tag{1}$$

Where T is the applied thrust, k is the torsional spring constant , d_{thr}, d_{capa} are the distance of thruster and displacement sensor from the balance rotational axis and θ_{final} is the steady state angular balance displacement for a constant thrust level. Since the angular displacement is sufficiently small ($<$ 1 mrad for maximum of the displacement sensor range) a measurement of the linear displacement $x_{\mathrm{final}} = \theta_{\mathrm{final}} \cdot d_{\mathrm{capa}}$ instead of the angular displacement can be done without introducing a large error. To measure thrust the two distances and the torsional spring constant need to be known. Alternatively a measurement with a voice coil of a known force constant can be done to determine a calibration factor for applied force vs. capacitive sensor voltage signal. With this calibration factor the thrust can be determined from:

$$T = U_{\mathrm{capa}} \cdot \frac{d_{\mathrm{cal}}}{d_{\mathrm{thr}}} \cdot r_{\mathrm{cal}} \cdot c_{\mathrm{vc}} \tag{2}$$

Where U_{capa} is the displacement sensor voltage signal and r_{cal} the calibration factor obtained from a measurement of the capacitive sensor voltage signal for different thrust

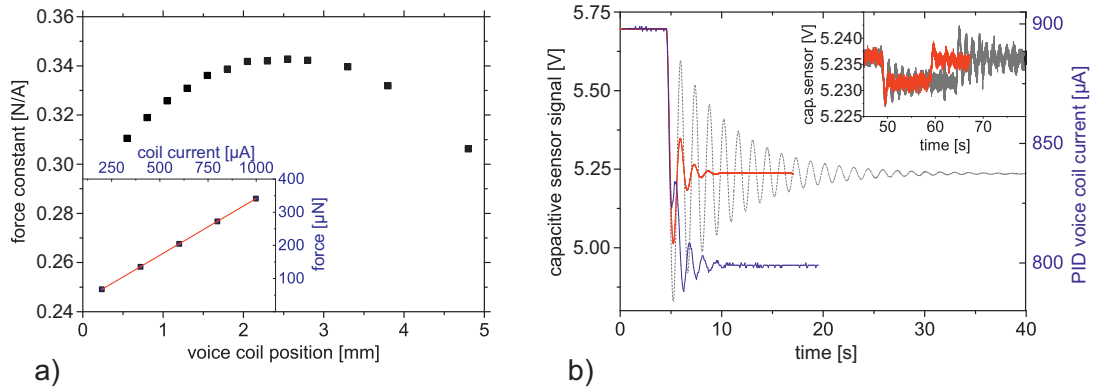

FIGURE 3. **a)** Voice coil calibration, Inset: linear force vs. current characteristic for one voice coil position; **b)** balance response examples for 100 μA step: capacitive sensor signal (left y-axis) for open-loop (gray), open-loop with active damping (red) and voice coil current (right y-axis) for closed-loop (blue) configuration; Inset: 1 μA step in open-loop with (red) and without (grey) active damping.

steps with a calibrated voice coil. Additionally the position of the calibration voice coil and thruster need to be determined. Voice coil and target position are known and thruster position is defined as the center of ablation area for the line scan ablation patterns that have so far been used in experiments.

For closed-loop operation the measured thrust can be determined from the voice coil calibration, the measured voice coil current I_{vc} and the thruster and coil positions: $T = \frac{d_{\mathrm{vc}}}{d_{\mathrm{thr}}} \cdot c_{\mathrm{vc}} \cdot I_{\mathrm{vc}}$. A second voice coil can be used to test PID operation and to provide an additional verification for closed-loop measurements.

Fig. 3 shows the balance response for open-loop (grey), open-loop with active damping (red) and closed-loop (blue) to a 100 μA current step and a 1 μA step applied to a calibrated voice coil with c_{vc}=0.342 μN/μA at l_{vc}= 125 mm on the balance arm. The measurements were done with the balance configuration shown in Fig. 2 (bottom) using a flexural pivot with a spring constant of 1.1 Ncm/rad. To reduce the time until steady state is reached variable active damping can be implemented with a second voice coil (see Fig. 3 red).

A new concept for balance calibration that also provides an alternative calibration mechanism for closed-loop operation has been tested. It is based on radiation pressure induced by a high power thin disk laser and a HR mirror fixed to one end of the balance arm. The radiation induced force F_{radiaton} on the balance is:

$$F_{\mathrm{radiaton}} = (1+R) \cdot \frac{P}{c} \cdot cos(\alpha) \tag{3}$$

where P is the optical power, R the mirror reflectivity, c the speed of light and α the angle of incidence. The calibration force is controlled by changing the pump diode

current where the smallest current step available from the power supply is 0.1 A.

Photon pressure calibration tests have been done in two different setups:

- Extra-cavity mode where the output beam is directed onto a HR-coated mirror (R > 99.98 %) located on the end of the balance arm at angle of incidence 10°. The reflected light is directed onto a powermeter (Ophir LW1500, power accuracy ±5%). In this case the photon pressure induced thrust can be calculated from the measured laser power P_{ext}, the angle of incidence and the mirror reflectivity. In this setup the maximum radiation force is 6.1 μN (equivalent to 930 W laser power) and the minimum force step is approx. 0.01 μN (equivalent to an approx. 2 W step for the smallest available current step of 0.1 A).
- Intra-cavity mode where the mirror fixed on the balance arm is one of the laser cavity mirrors. Because of the much higher intra-cavity optical powers this results in a much broader calibration force range of up to 240 μN. The optical power on the balance mirror is calculated from a measurement of the extra cavity laser power $P_{\text{int}} = P_{\text{ext}} \cdot \frac{1-T}{T}$, where T is the output coupler transmission, which was set to 2.4 %. To enable both closed- and open-loop calibration measurements the thin disk laser resonator has been designed to accommodate angular mirror displacement of up to approx. 2 mrad.

For first tests the thrust balance was moved to a different lab where a laminar flow cabinet was available. Instead of the vacuum chamber it was placed inside an enclosure to limit the influence from air flow, however the remaining influence of the air flow and the different lab environment resulted in a higher noise level. Results from first measurements for both intra- and extra-cavity mode are shown in Figure 4. To test this method of thrust balance calibration the induced thrust was both determined by calculating the thrust from measurements of the calibration laser power (red) and from either the voice coil current for closed-loop or from balance parameters for open-loop (black lines). They show good agreement within the accuracy ±5% for the laser power measurement (Ophir LW1500).

Surface Diagnostics

A commercial white light interferometer (Veeco NT9100) is used for analysis of the target surface for different purposes:

- 3D-measurements of crater geometry for an approximation of ablated volume and as a result ablated mass.
- To provide information on the target surface roughness before and after ablation.
- For positioning and adjustment purposes: positioning of the targets in the focus by moving the focusing lens on a micrometer and ablating on an unablated spot for each position and also for choosing the appropriate step size for target positioning or scanning speed for beam-steering in thrust measurements.

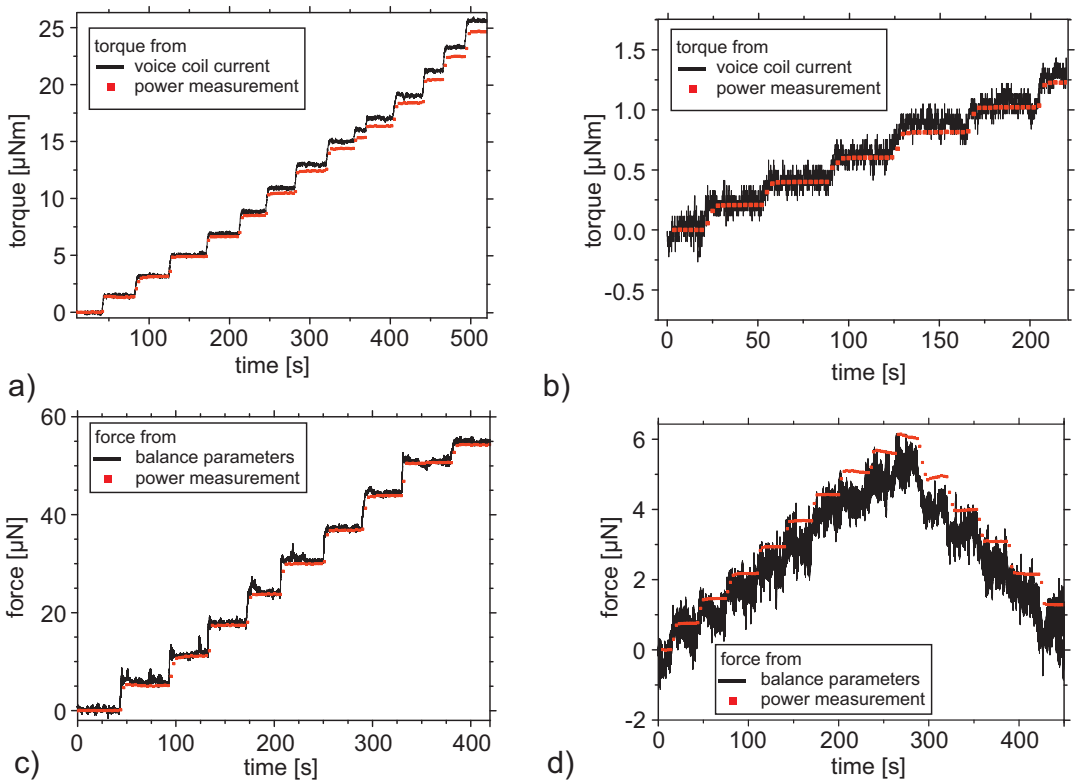

FIGURE 4. Results for radiation pressure calibration tests for: **a)** intra-cavity closed-loop (max. 320 W), **b)** extra-cavity closed-loop (max. 676 W), **c)** intra-cavity open-loop (max. 200 W) and **d)** extra-cavity open-loop (max. 930 W).

- To determine the exact position of the ablation pattern for thrust measurements.

Ablation Diagnostics

Analysis of the plasma plume that results from each ablation event is useful for gaining a better understanding of the laser ablation process, assessing the influence of changing surface roughness and for evaluation of contamination issues. In the current experimental setup information on charged plume components can be obtained from Faraday cup measurements. An overview of the setup is given in Fig. 5. The beam from a microchip laser is directed into an approx. 35 l vacuum chamber via an adjustable attenuator and is focused onto the sample. Measurements are usually done at $< 5 \cdot 10^{-6}$ mbar, which can be achieved after short pump down times with a 15 m^3/h scroll pump and a 1550 l/s N_2 turbomolecular pump vacuum system. A reflection from an uncoated wedge is split off for pulse energy monitoring and to provide a trigger signal for the Faraday cup measurements. The target is fixed on a motorized x,y-stage setup, which can be used to move the target to a virgin spot for each ablation event

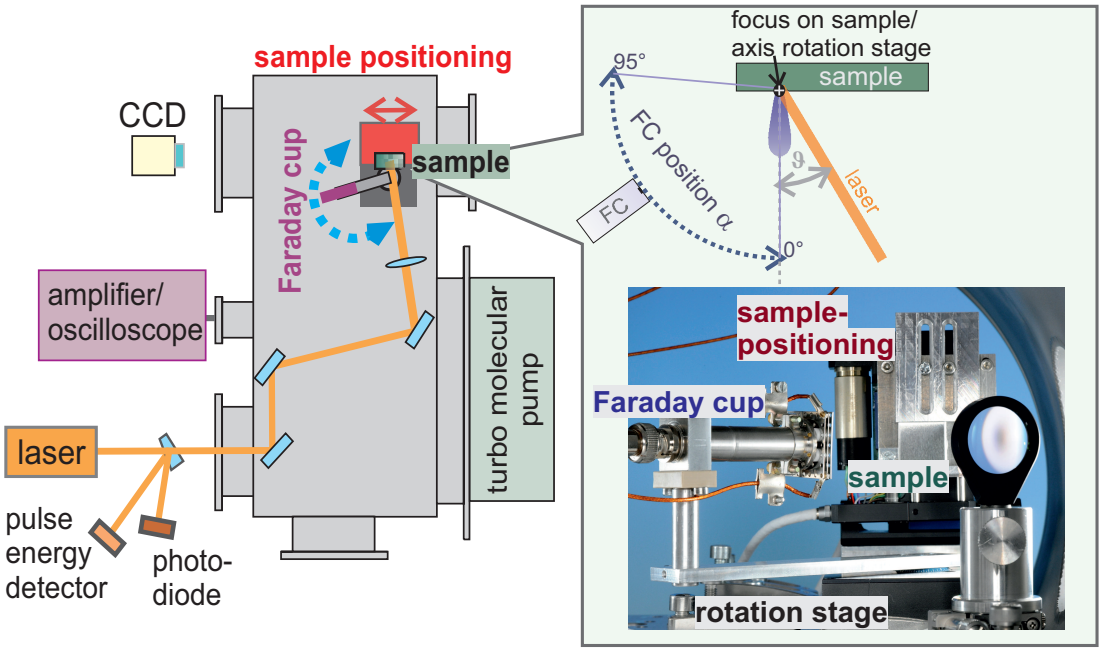

FIGURE 5. Faraday cup ablation diagnostics setup. FC: Faraday cup, ϑ: Faraday cup angular position, α: laser angle of incidence.

or to implement different overlap patterns. Positively charged plume components are collected with a negatively biased 5 mm Ø aperture Faraday cup and the amplified signal is read out on an oscilloscope (LeCroy, WaveSurfer 104MXs-B). For measurements at different angular positions the Faraday cup is mounted on a rotational stage with its rotational axis centered at the focus point on the sample (see Fig. 5). As shown in Fig. 6 b, single shot Faraday cup measurements for the same parameters on an unablated spot show good agreement both perpendicular to the sample (α=0°) and at different angles. In the current setup in the 35 l vacuum chamber the variation of angles of incidence is limited to max. ϑ=30° and the position of the Faraday cup can be varied between 95°<α<0°. Measurements have been automated in LabView.

A first test to use the coating formed on a transparent substrate after many single shot ablation events has also been carried out. Unlike Faraday cups this method yields information on all plume components and has already been successfully employed, however, for vastly laser parameters [15, 16]. For this purpose a PTFE foil substrate with a hole for passing the laser beam was fixed on a curved mount with 1.25 mm radius that was centered on the ablation point on the sample (see Fig. 6 a). Deposit from 300.000 shots (laser parameters: 71.7 μJ, 1064 nm, 500 ps, ϑ=15°) on an Al target was collected and analyzed on a flatbed scanner with a transmitted light unit (Epson V700). Reflective ND Filters with an OD of down to 0.1 were also scanned. The result is shown Fig. 6 a. While a greyscale gradient for the deposited material could be obtained a calibration with ND filters similar to [15] would require a much larger amount of deposit since the transmission of the darkest area of the coating was still much higher than for an OD 0.1 filter.

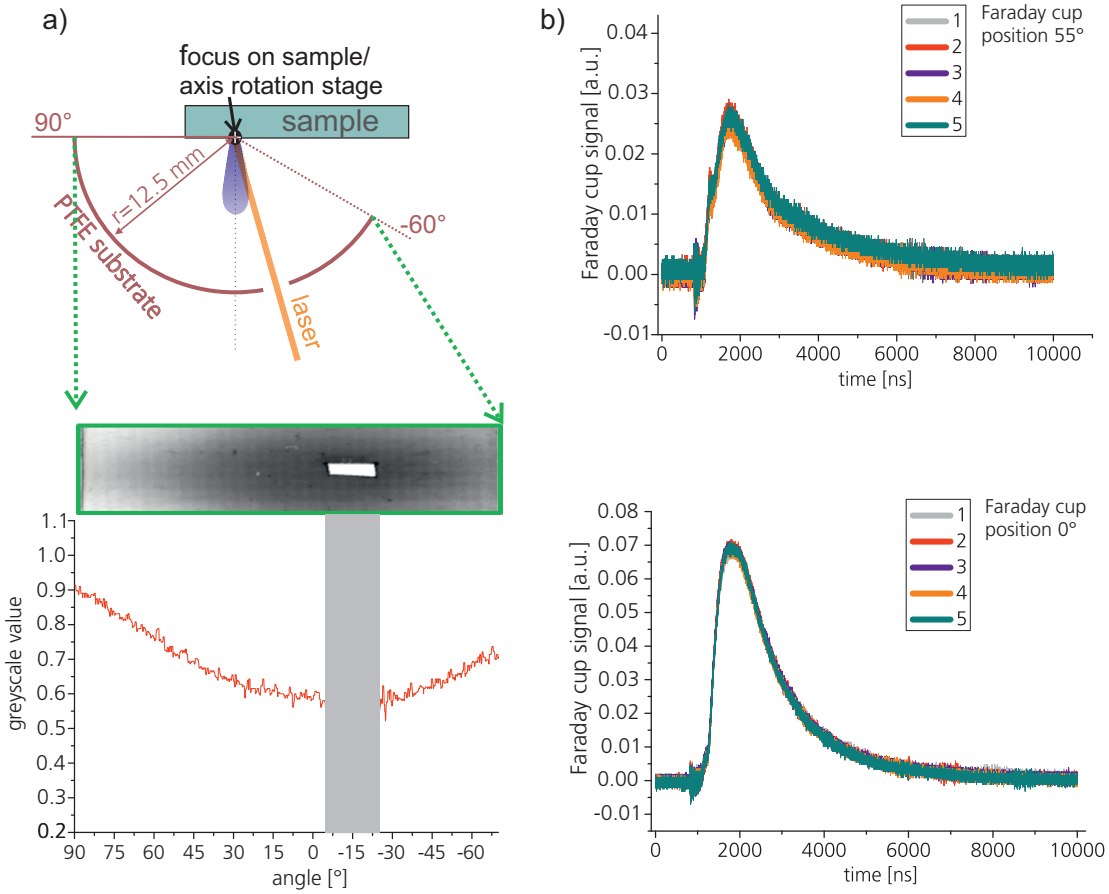

FIGURE 6. **a)** Setup for and result for PTFE coating test; **b)** comparison of several single shot Faraday cup signals for Cu samples and laser parameters 500 ps, 1064 nm, 71.7 mJ, p-polarization, 15° angle of incidence, Faraday cup positions: α=0° (bottom) and α=55° (top).

4 SUMMARY AND OUTLOOK

Experimental facilities that allow for a variation of a range of relevant parameters have been set up for the investigation of the potential of a laser ablative microthruster concept. The available lasers allow for variation of pulse energies from μJ to several mJ and pulse lengths between 500 ps to 10 ns. For micropropulsion measurements target materials have so far been high purity Cu and Al with good surface quality. The next step in investigating the influence of these parameters will be experiments with shorter pulses closer to material-specific electron-phonon coupling times [7] and experiments on the influence of the ablation pattern and surface quality. The ablation pattern is controlled by either moving the target, which is appropriate for ablation diagnostics where a fixed focus position is required, or by using a galvanometer mirror beam-steering mechanism, which is necessary for thrust measurements. Currently the potential

of 1D KTN crystal based beam scanners (NTT) [17] for providing a basis for a 2D electro-optical beam scanning mechanism is being investigated. Experimental facilities that provide information on the relevant figures of merit have originally been set up for micropropulsion experiments but can, because of their flexibility, also be used for debris removal relevant experiments. A torsional pendulum thrust balance with an adaptable design can measure steps down to sub μN and with the available DC power source up to several mN in closed-loop operation. A radiation pressure based calibration concept using a kW thin disk laser has been tested as an alternative for thrust balance calibration with voice coils. Here the next step will be tests of single shot measurements with a higher pulse energy laser and adapting the set up for different angles of incidence for space debris removal measurements. Faraday cups provide information on the angular distribution of charged plume components and a first test for analyzing the deposit of all plume components on a transparent substrate has been carried out. For the Faraday cup setup the next step will be to expand the limited range of the Faraday cup positions to a full 180° range by moving the setup to the bigger vacuum chamber. This should give more conclusive information on the influence of surface geometry and angle of incidence on the charged plume component, which is of interest both for space debris and microthruster related measurements.

ACKNOWLEDGMENTS

Technical support form the Institute of Technical Physics' mechanical and electronics workshops is gratefully acknowledged. The authors would also like to thank J. Mende for contributing the calibration laser design and C. Illg, S. Scharring, D. Sperber, D. Förster for their scientific contributions and helpful discussions.

REFERENCES

1. B. Esmillier, CLEANSPACE - Space Debris Removal by Ground Based Laser: Progress of the European Project , Presentation at the International Symposium on High Power Laser Ablation and Beamed Energy Propulsion, Santa Fe, NM, 2014, submitted to these proceedings (2014).
2. C. P. E. Early, C. Bibeau, "Space debris de-orbiting by vaporization impulse coupling using short pulse laser," in 2st *International Symposium on Beamed Energy Propulsion*, edited by A. V. K. Komurasaki, AIP Conference Proceedings 702, American Institute of Physics, Melville, New York, 2003, pp. 190–201.
3. D. A. Gonzales, and R. P. Baker, "Micropropulsion using a Nd:YAG microchip laser," in *High-Power Laser Ablation IV*, edited by C. R. Phipps, Proceedings of SPIE 4760, SPIE, Taos, NM, USA, 2002, pp. 752–765.
4. C. R. Phipps, J. R. Luke, W. Helgeson, and R. Johnson, "Performance test results for the laser-powered microthruster," in 4th *International Symposium on Beamed Energy Propulsion*, edited by K. Komurasaki, AIP Conference Proceedings 830, American Institute of Physics, Melville, New York, 2006, pp. 224–234.
5. C. R. Phipps, J. R. Luke, and W. D. Helgeson, "3ks Specific Impulse with a ns-pulse Laser Microthruster", in 29th *International Electric Propulsion Conference*, IEPC paper 2005-319 (2001).
6. C. R. Phipps, J. R. Luke, and W. Helgeson, "Liquid-fueled, laser-powered, N-class thrust space engine with variable specific impulse," in 5th *International Symposium on Beamed Energy Propulsion*, edited by A. V. Pakhomov, AIP Conference Proceedings 997, American Institute of Physics, Melville, New York, 2008, pp. 222–231.

7. H.-A. Eckel, S. Scharring, S. Karg, C. Illg, and J. Peter, Overview of Laser Ablation Micropropulsion Research Activities at DLR Stuttgart , Presentation at the International Symposium on High Power Laser Ablation and Beamed Energy Propulsion, Santa Fe, NM, 2014, submitted to these proceedings (2014).
8. B. Esmiller, and C. Jacquelard, “CLEANSPACE Small Debris Removal by Laser Illumination and Complementary Technologies,” in 7^{th} *International Symposium on Beamed Energy Propulsion*, edited by S. S. H.-A. Eckel, AIP Conference Proceedings 1402, American Institute of Physics, Melville, New York, 2011, pp. 347–353.
9. Online simulation accessible at:, http://vll.ihed.ras.ru/ (last accessed April 2014).
10. J. K. Ziemer, "Performance Measurements Using a Sub-Micronewton Resolution Thrust Stand", in 27^{th} *International Electric Propulsion Conference*, IEPC paper 2001-238 (2001).
11. C. R. Phipps, J. R. Luke, W. Helgeson, and R. Johnson, “A low-noise thrust stand for microthrusters with 25 nN resolution,” in 4^{th} *International Symposium on Beamed Energy Propulsion*, edited by K. Komurasaki, AIP Conference Proceedings 830, American Institute of Physics, Melville, New York, 2006, pp. 492–499.
12. M. Gamero-Castaño, V. Hruby, and M. Martinez-Sánchez, "A Torsional Balance that Resolves Sub-micro-Newton Forces", in 27^{th} *International Electric Propulsion Conference*, IEPC paper 2001-235 (2001).
13. A. D. Ketsdever, B. C. D’Souza, and R. H. Lee, *Journal of Propulsion and Power* **24**, 1376–1381 (2008).
14. H. Koizumi, K. Komurasaki, and Y. Arakawa, *Review of Scientific Instruments* **75**, 3185–3190 (2004).
15. T. Donnelly, J. G. Lunney, S. Amoruso, R. Bruzzese, X. Wang, and X. Ni, *Applied Physics A* **100**, 569–574 (2010).
16. M. Keidar, I. D. Boyd, J. Luke, and C. Phipps, Plasma generation and plume expansion for a transmission-mode micro-laser ablation plasma thruster, 39th AIAA/ASME/SAE/ASEE Joint Propulsion Conference and Exhibit 20-23 July 2003, Huntsville, Alabama (2003).
17. K. Nakamura, J. Miyazu, M. Sasaura, and K. Fujiura, *Applied Physics Letters* **89** (2006).